Aust. J. Phys., 1983, **36**, 401–15

H_2O Masers in the Galactic Plane. I Longitude 340° to the Galactic Centre

J. L. Caswell, R. A. Batchelor, J. R. Forster and K. J. Wellington

Division of Radiophysics, CSIRO, P.O. Box 76, Epping, N.S.W. 2121.

Abstract

Twenty-five new H_2O masers in the southern galactic plane have been discovered using a 22 GHz maser receiver on the Parkes telescope. The search was conducted at the locations of all the known 1665 MHz OH masers in the longitude range 340° through the galactic centre to 2°; of the 46 type I OH masers 38 are now found to have an H_2O maser nearby; three other main-line OH emitters, possibly unusual late-type stars, also show H_2O emission. We give an up-to-date tabulation of all 46 currently known H_2O masers in the region which includes for completeness several H_2O masers with no readily detectable associated type I OH emission.

Although a few very active regions of star formation harbour several masers, most commonly there is one, and usually only one, site of H_2O maser emission near each OH maser. In a few well-investigated instances an H_2O maser is found to be slightly displaced spatially from its OH maser counterpart; this fact leads us to propose a 'binary' origin for such displaced pairs (perhaps applicable to most other H_2O/OH pairs) in which the OH maser/compact HII region/new star is one of the pair, and a dense molecular cloud of stellar mass, not necessarily undergoing transformation to a star, is the other component giving rise to the H_2O emission.

1. Introduction

In recent years the Parkes 64 m radio telescope has been used to conduct extensive searches for maser emission from the 1665 MHz transition of the hydroxyl radical. The survey results for the galactic plane from longitude $l = 340°$ to the galactic centre, which have now been completed (Caswell and Haynes 1983; referred to as CH 83, see present issue p. 361), led to the detection of 49 OH main-line masers, the majority of which were new discoveries. Such OH masers are usually at the periphery of ultra-compact HII regions that surround newly formed O and B stars. An important question is whether the H_2O masers sometimes found near these sites of new star formation are *invariably* present in association with the OH masers. We have attacked this question on the statistics of such associations by searching for H_2O masers at all the known OH maser positions. The high sensitivity necessary for such a project has been accomplished using a new maser receiving system on the Parkes radio telescope.

Our detection of many weak new H_2O masers also provides a useful sample for the study of their general properties.

0004-9506/83/030401$02.00

2. Observations

Earlier observations of H_2O masers at 22 GHz using the Parkes telescope were summarized by Batchelor *et al.* (1980; referred to as B+80). In the present observations (1981 December and 1982 April), we again illuminated the central 37 m portion of the telescope to yield a beam size to half-power of 100″ arc and a ratio of flux density to antenna temperature of 9 Jy K^{-1}. However, a new maser receiver constructed at the CSIRO Division of Radiophysics provided an improvement in sensitivity of an order of magnitude compared with earlier receivers; in good observing conditions the system temperature was as low as 60 K. A 1024-channel correlator was used in a mode which gave three overlapping 10 MHz spectra and a total coverage of 24 MHz (320 km s^{-1}). The central 10 MHz band employed 512 channels to give a velocity resolution (after Hanning weighting) of 0·53 km s^{-1} (40 kHz) and the outer bands employed 256 channels each to give a velocity resolution (uniform weighting) of 0·64 km s^{-1}.

The flux density scale is relative to Jupiter, assumed to have a brightness temperature of 140 K, uniform over its optical disk; atmospheric attenuation corrections were applied to all observations and typically amounted to 10% at the zenith. Since all observations were made using a linearly polarized feed (with the *E* plane aligned vertically), in all remarks on variability we implicitly assume that any linear polarization is small (see Knowles and Batchelor 1978).

Search observations at the OH position were generally 5 min integrations on-source combined with 5 min off-source (band-pass reference) integrations. Our sensitivity, at the 3σ detection level, was between 1 and 2 Jy (1 Jy $\equiv 10^{-26}$ W m^{-2} Hz^{-1}), depending on weather conditions and telescope elevation angle.

Upon discovery of an H_2O source, a more accurate position was determined in most cases using a grid of four observations surrounding the discovery position. Residual r.m.s. errors in our estimate of each source position are ~12″ arc in each coordinate.

3. Results

A summary of results is presented in Table 1. To avoid unnecessary duplication, we use the same table both to list the H_2O maser data *and* to list those OH maser positions where only upper limits to any H_2O emission were obtained. Column 1 gives the galactic coordinates of the H_2O maser and columns 2 and 3 give the equatorial (1950) positions. Column 4 gives the velocity of the most prominent feature, and column 5 its approximate width to half intensity; where the velocity structure is complex it is necessary to consult Figs 1–3 and the subsequent notes. References and comments on previous H_2O measurements are given in column 7. Column 8 lists the associated OH maser, drawn from CH 83.

Figs 1–3, which show spectra of many of the sources, cover only the central portion of the velocity range observed; in all cases illustrated, the outlying regions of the spectra showed no emission above the noise level. The notes below give further detailed comments on the H_2O maser sources, and following these notes are some remarks on the OH sources where no H_2O maser was detected. Comments on associated HII regions and continuum emission in general are based on the 5 GHz survey of Haynes *et al.* (1978).

H_2O 339·68−1·21 and H_2O 339·88−1·26 (*Fig. 1*). These sources are associated with recently discovered OH masers (CH 83). No HII regions have been detected (Haynes *et al.* 1978). They are probably at near kinematic distances in view of the considerable offsets from the galactic equator.

H_2O 340·06−0·24 (*Fig. 1*). This was detected by B+80 in 1976 August, at which time the intensity was too low (7 Jy) to allow a position measurement. Scalise and Braz (1980) measured a peak intensity of 14 Jy in 1978 September. At the epoch of our measurement (1981 December) the peak intensity was 40 Jy and a position measurement was made. The offset from the associated source OH 340·06−0·25 is not significant (being 26″ arc, less than the combined errors).

H_2O 341·21−0·21 (*Fig. 1*). The weak emission at $v = -52$ km s^{-1} was confirmed in an independent integration.

H_2O 342·01+0·25. This maser has been studied by Braz and Scalise (1982) and by Sandell *et al.* (1983); we have no new H_2O observations but include it for completeness. An OH counterpart shows 1612 and 1667 MHz emission (Caswell *et al.* 1981) and is not readily classified; it may be either a type I maser or possibly an unusual late-type star, and we exclude it from the type I OH source statistics.

H_2O 343·12−0·06. No new observations have been made since the discovery measurement (1977 May) by B+80. A weak feature at $v = -20$ km s^{-1}, offset by 14 km s^{-1} from the main emission, is probably best regarded as 'high-velocity' emission.

H_2O 343·93+0·12. Both the OH maser and the H_2O maser are quite weak and have no clearly associated HII emission. The kinematic distance is 19·5 kpc; a near distance of less than 1 kpc is possible if small non-circular motions are present but the weakness of the masers is a slight argument in favour of the far position.

H_2O 344·23−0·57 (*Fig. 1*). First discovered (1978 June) by Scalise and Braz (1980). Our measured intensity of the main feature in 1981 December is similar and our larger velocity coverage has led to the detection of a high-velocity feature near $v = +10$ km s^{-1}. We have measured an improved position which agrees well with the OH maser position. The OH maser is somewhat unusual in exhibiting emission which is stronger at 1667 MHz than at 1665 MHz. A compact HII region with $S = 1·7$ Jy is associated with the masers.

H_2O 344·58−0·03 (*Fig. 1*). This is the strongest of our new H_2O masers; it is associated with a strong new OH maser. Weak high-velocity emission is present.

H_2O 345·00−0·23 (*Fig. 1*). The associated OH maser is noteworthy in that the main-line emission is accompanied by very strong 1720 MHz emission.

H_2O 345·01+1·80 and H_2O 345·01+1·79 (*Fig. 1*). These two H_2O masers are separated by 37″ arc and straddle the OH maser position; the spectrum shows both sources and was taken nearer the position of the weaker source H_2O 345·01+1·80, where the response to the other source is reduced by a factor of 0·79. The weaker source has a velocity closer to that of the OH maser, and also apparently lies closest to the OH position, although the errors leave some uncertainty about this latter conclusion. The masers are associated with an extended HII region, and the distance of the complex is probably less than 3 kpc.

H_2O 345·41−0·94. Previous results are summarized by B+80. In 1981 December we failed to detect H_2O 345·41−0·94, the upper limit of 2 Jy being well below the

1983AuJPh..36..401C

Table 1. H_2O masers and associated OH masers in the galactic longitude range 340° to 360° to 2°

(1) H_2O maser l °	b °	(2) Position (1950) R.A. h m s	(3) Dec. ° ′ ″	(4) Radial velocity (km s^{-1})	(5) Velocity width (km s^{-1})	(6) Peak intensity (Jy)	(7) H_2O reference and remarks[A]	(8) OH maser l °	b °
H_2O 339·68−1·21		16 47 25·3	−46 11 03	−28	See Fig. 1	15	New	OH 339·68−1·21	
H_2O 339·88−1·26		16 48 26·5	−46 03 48	−37	See Fig. 1	100	New	OH 339·88−1·26	
H_2O 340·06−0·24		16 44 36·4	−45 16 26	−53	See Fig. 1	40	B+80; new position measured	OH 340·06−0·25	
—		—	—	—	—	<2		OH 340·78−0·10	
H_2O 341·21−0·21		16 48 40·6	−44 22 07	−41	See Fig. 1	136	New	OH 341·21−0·21	
—		—	—	—	—	<2		OH 341·27+0·07	
H_2O 342·01+0·25[B]		(16 49 31·1)	(−43 27 40)	−44		~34	BS 82; OH position assumed	OH 342·01+0·25	
H_2O 343·12−0·06		16 54 42·8	−42 47 49	−34	2	100	Data from B+80	OH 343·12−0·06	
H_2O 343·93+0·12		(16 56 39·1)	(−42 02 58)	+9	~5	2	New; OH position assumed	OH 343·93+0·12	
H_2O 344·23−0·57		17 00 36·0	−42 14 32	−28	See Fig. 1	78	SB 80; new position measured	OH 344·22−0·57	
—		—	—	—	—	<2		OH 344·41+0·05	
H_2O 344·58−0·03		16 59 28·5	−41 37 47	−4	See Fig. 1	789	New	OH 344·58−0·02	
H_2O 345·00−0·23		17 01 40·7	−41 25 07	−23	See Fig. 1	92	New	OH 345·00−0·22	
H_2O 345·01+1·80		16 53 18·8	−40 09 36	−20	See Fig. 1	15	New	} OH 345·01+1·79	
H_2O 345·01+1·79		16 53 21·7	−40 09 51	−10	See Fig. 1	57	New		
H_2O 345·41−0·94		17 06 02·3	−41 31 44	−22	~1	30	Data from B+80	OH 345·4−0·9	
H_2O 345·51+0·35		17 00 53·6	−40 40 02	−28	1·5	530	Data from B+80	OH 345·51+0·35	
H_2O 345·64+0·01[B]		(17 02 48)	(−40 45 26)	−9	~2	57	Data from BS 82	—	
H_2O 345·69−0·09		17 03 19·7	−40 47 31	−9		290	Data from B+80	OH 345·70−0·09	
—		—	—	—	—	<2		OH 346·48+0·13	
H_2O 347·63+0·15		(17 08 23·9)	(−39 05 50)	−100	2·5	2·1	OH position assumed	OH 347·63+0·15	
—		—	—	—	—	<2		OH 347·87+0·01	
H_2O 348·22+0·46[B]		(17 08 39)	(−38 27 06)	−11		27	Data from BS 82	? see text	
H_2O 348·55−0·98		17 15 53·1	−39 00 57	−15	See Fig. 2	9	New	OH 348·55−0·97	
H_2O 348·73−1·04		17 16 39·7	−38 54 17	−11		390	Data from B+80	OH 348·73−1·06	
? see text		—	—	—	—	<2?	Possible detection	OH 348·89+0·09	
H_2O 348·89−0·18		17 13 35·2	−38 16 18	+8	See Fig. 2	15	New	OH 348·89−0·19	
H_2O 349·07−0·02		17 13 25·5	−38 01 56	+6	~1	4·7	New	OH 349·07−0·01	

H_2O 349·09+0·11	17 12 58·4	−37 56 21	−81	~1	370	Data from B+80	OH 349·09+0·11
H_2O 350·01+0·43	17 14 23·1	−37 00 21	−39	See Fig. 2	13	New	OH 350·02+0·43
H_2O 350·10+0·09	17 16 01·0	−37 07 30	−66	~2	3·2	New	OH 350·11+0·09
H_2O 351·16+0·70	17 16 34·5	−35 54 44	−6	2·5	20	Data from B+80	OH 351·16+0·70
H_2O 351·24+0·66[B]	(17 16 58·3)	(−35 51 50)	−80	4	2300	Data from R+78; B+80	—
H_2O 351·41+0·64	17 17 32·5	−35 44 13	−9	~2	3200	Data from B+80	OH 351·41+0·64
H_2O 351·58−0·36	17 22 04·2	−36 10 11	−100	See Fig. 2	47	New	OH 351·58−0·35
H_2O 351·77−0·54	17 23 20·9	−36 06 53	−1	See Fig. 2	679	BS 82 plus new data	OH 351·78−0·54
—	—	—	—	—	<2		OH 352·16+0·21
H_2O 352·52−0·16	17 23 51·2	−35 17 03	−46	See Fig. 2	2·7	New	OH 352·51−0·15
H_2O 353·41−0·36	17 27 06·5	−34 39 41	−14	~5	45	Data from B+80	OH 353·41−0·36
H_2O 353·46+0·55	17 23 34·2	−34 06 38	−52	~2	4·9	New	OH 353·45+0·54
H_2O 354·61+0·47	17 27 00·6	−33 11 47	−11	See Fig. 2	12	New	OH 354·61+0·48
H_2O 355·34+0·14	17 30 14·0	−32 46 07	+10	See Fig. 2	59	New	OH 355·34+0·15
H_2O 356·64−0·33[B]	17 35 26·1	−31 56 00	−10	~3	20	Data from B+80	OH 356·64−0·32
—	—	—	—	—	<2		OH 356·66−0·27
H_2O 358·23+0·11[B]	17 37 41·7	−30 21 17	−10	See Fig. 3	82	New	OH 358·23+0·11
H_2O 358·67−0·05[B]	17 39 23·5	−30 04 30	−21	See Fig. 3	60	New	OH 358·66−0·06
H_2O 359·14+0·03	17 40 15·5	−29 38 08	−2	See Fig. 3	367	New	OH 359·14+0·03
H_2O 359·43−0·11	17 41 29·8	−29 27 13	−59	See Fig. 3	16	New	OH 359·43−0·10
H_2O 359·62−0·25	17 42 30·0	−29 22 25	+13	See Fig. 3	12	New	OH 359·62−0·25
H_2O 359·97−0·46	17 44 10·4	−29 11 03	+21	See Fig. 3	32	New	OH 359·97−0·46
H_2O 0·37+0·04	17 43 11·0	−28 34 40	+39	See Fig. 3	36	New	OH 0·37+0·04
H_2O 0·54−0·85	17 47 03·2	−28 53 54	+18	~2	60	Data from B+80	OH 0·54−0·85
H_2O 0·66−0·04	17 44 10·6	−28 22 39	+63	~1	1000	Sgr B2; data from GD 77	OH 0·66−0·04
H_2O 2·14+0·01	17 47 28·3	−27 05 12	+62	See Fig. 3	15	New	OH 2·14+0·01

[A] References: B+80, Batchelor *et al.* (1980); BS 82, Braz and Scalise (1982); SB 80, Scalise and Braz (1980); R+78, Rodriguez *et al.* (1978); GD 77, Genzel and Downes (1977).

[B] Not included in the sample used to investigate the association with type I OH masers; see Section 3.

1976 intensity of 30 Jy. The associated OH maser is weak and its position has a quite large uncertainty of ~60″ arc.

H_2O 345·51+0·35. Previous results were summarized by B+80; no new H_2O data are available.

H_2O 345·64+0·01. This was discovered by Braz and Scalise (1982). There is apparently no associated OH maser, the nearest one being OH 345·69−0·09, which has a much closer associated H_2O maser (see next note).

H_2O 345·69−0·09. Previous results were summarized by B+80. A new observation (1981 December) showed the same two main features at $v = -8{\cdot}8$ and $-4{\cdot}4$ km s^{-1}, with intensities of 415 and 217 Jy (50% larger than in 1976 August), and a weak feature of 9 Jy is now present at $-18{\cdot}5$ km s^{-1}.

H_2O 347·63+0·15. An H_2O maser with $v = -84$ km s^{-1} was first reported near this position by Kaufmann *et al.* (1977) with an intensity of 49 Jy in 1975 November, falling to 20 Jy in 1976 May. Our 1981 December observations showed no emission near -84 km s^{-1} (<1 Jy) but a weak feature of 2·1 Jy was found at $v = -100$ km s^{-1}. The observation was made at the OH position, with no direct measurement of the H_2O position; however, the velocity is in quite good agreement with that of the OH maser (which covers the range -99 to -92 km s^{-1}). The corresponding kinematic distance is large, near the tangential point, at 9·7 kpc.

H_2O 348·22+0·46. This was discovered by Braz and Scalise (1982), in the direction of a weak 1665 MHz OH maser reported by Turner (1970). Subsequent OH observations (Turner 1979; Caswell and Haynes, unpublished data) have failed to confirm the OH maser, and since Turner's original 'detection' was below the 3σ level of his survey and had a velocity displaced from the H_2O emission, the source may have been spurious. However, OH *absorption*, with $v = -8$ km s^{-1}, is definitely present at both 1665 and 1667 MHz, and this OH cloud is presumably associated with the H_2O maser and the HII region RCW 120.

H_2O 348·55−0·98 (*Fig. 2*). This is a new H_2O maser associated with an OH maser in a nearby strong HII region.

H_2O 348·73−1·04. This is an H_2O maser with a high-velocity feature, as discussed by B+80; no recent observations are available.

H_2O 348·89−0·18 (*Fig. 2*). Both this new H_2O maser and the associated OH maser (348·89−0·19) are centred at a small positive velocity, and a weak (0·4 Jy at 5 GHz) continuum source coincides in position. It is not clear whether the complex is very near or at ~20 kpc; the implied luminosity at the latter distance is large but by no means excessive.

H_2O 349·07−0·02. As in the case of the previous source, the new H_2O maser and the OH maser (349·07−0·01) are centred at a small positive velocity; they are associated with a weak HII region and the complex may be at the far distance of ~20 kpc.

H_2O 349·09+0·11. H_2O emission was summarized by B+80. The H_2O/OH/HII region complex is at a distance of 9·8 kpc.

Figs 1–3. Spectra of H_2O masers. The source names and observing dates are shown within each frame. The velocity resolution is 0·53 km s^{-1} (40 kHz).

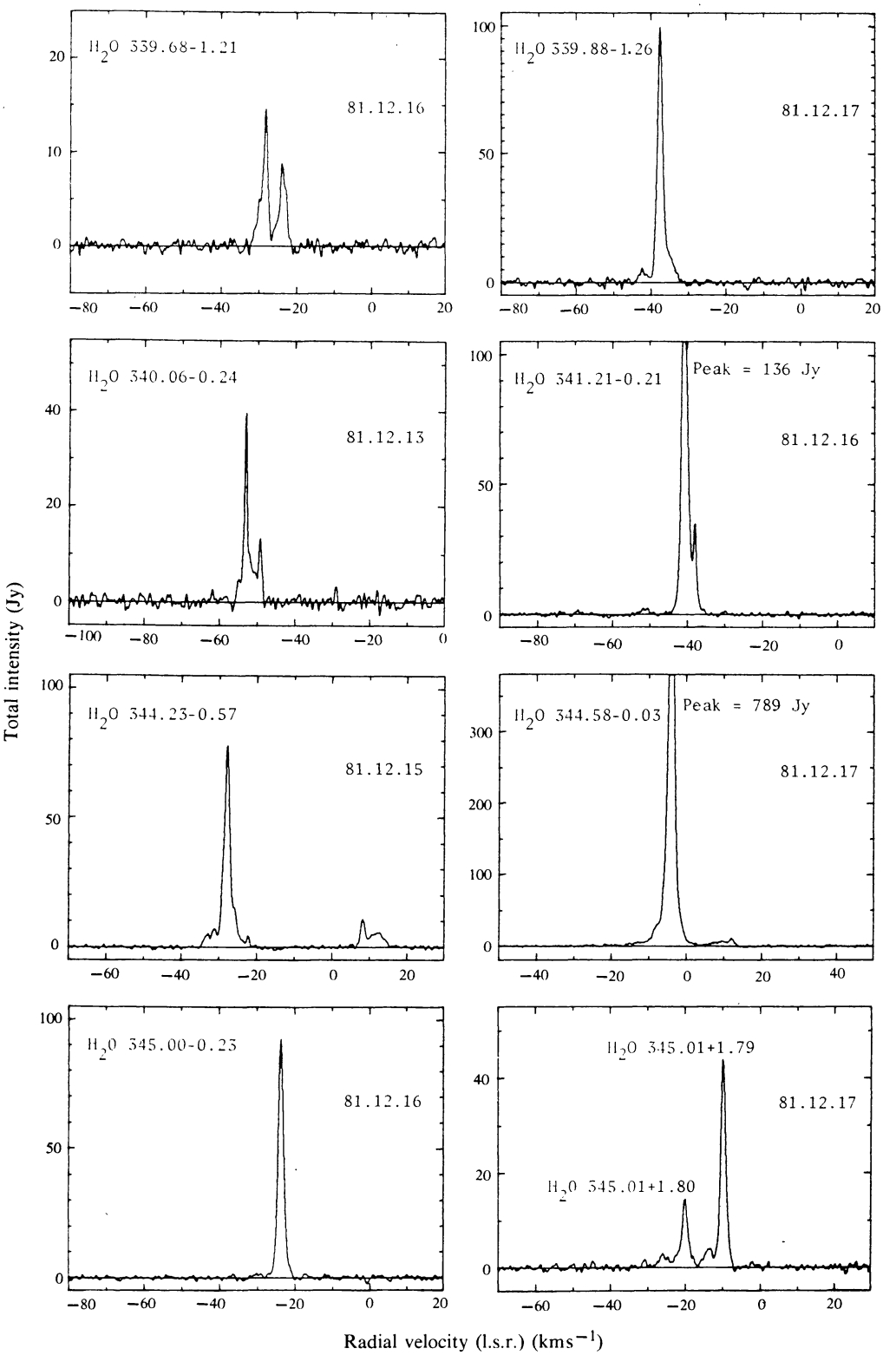

Fig. 1

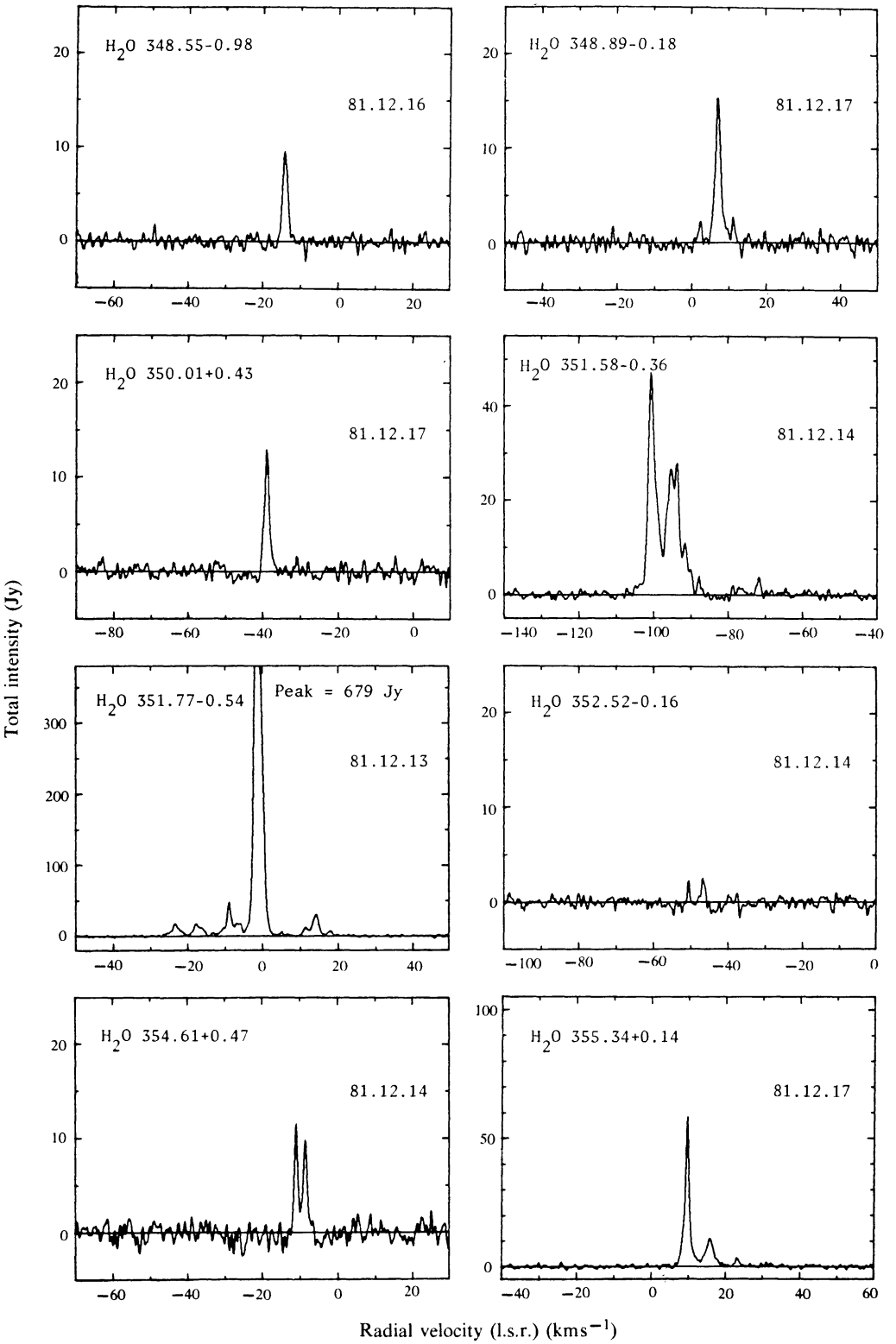

Fig. 2

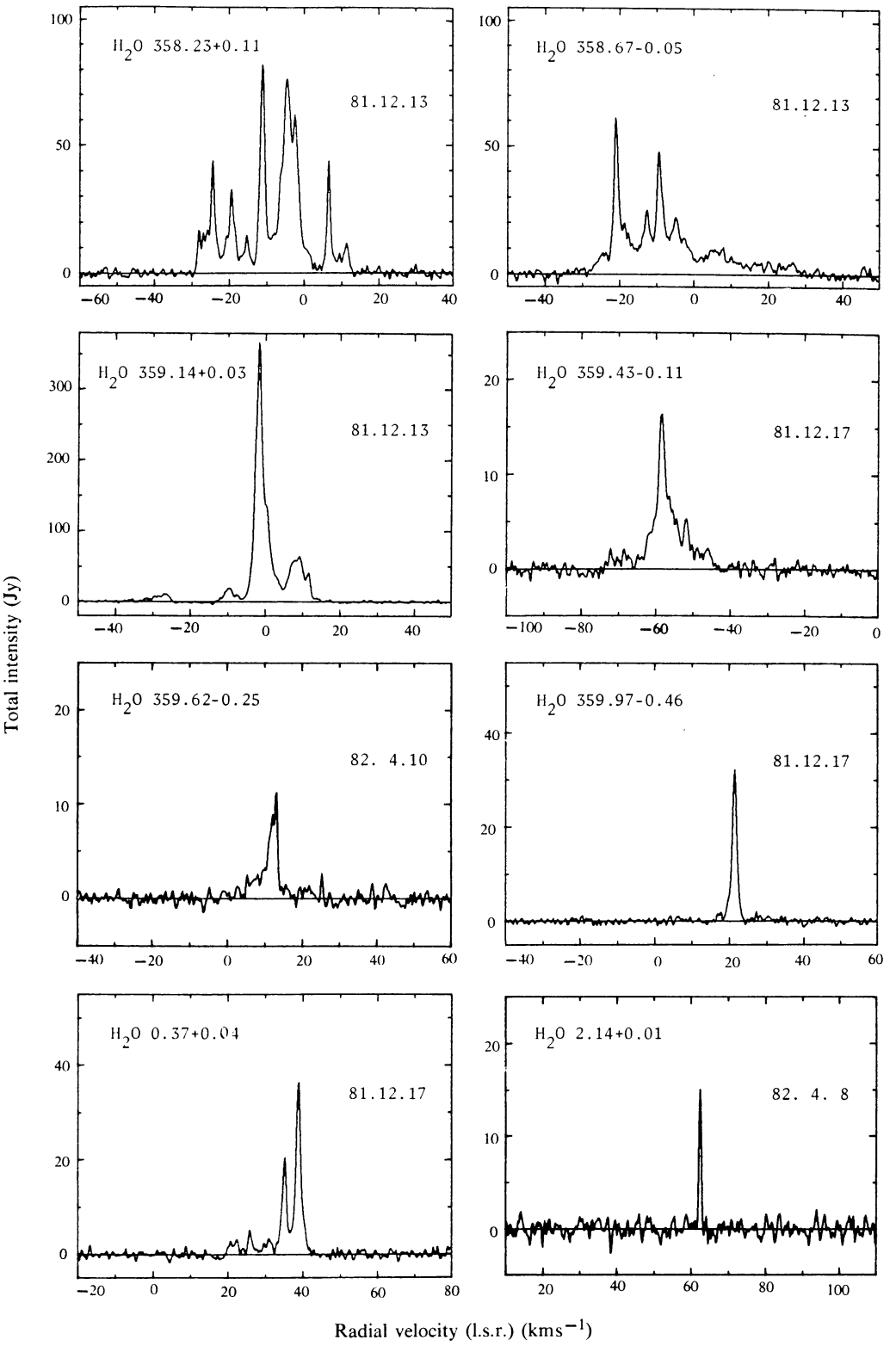

Fig. 3

H_2O 350·01+0·43 (*Fig. 2*). This is a new H_2O maser with a weak OH maser counterpart and coinciding with a compact continuum source (S_5 = 0·6 Jy).

H_2O 350·10+0·09. This new H_2O maser is very weak and is associated with a strong OH maser and HII region, at a distance of ~10 kpc.

H_2O 351·16+0·70 and H_2O 351·41+0·64. These well-known sources, each with an associated OH maser, lie in the HII regions NGC 6334B and NGC 6334A respectively. The H_2O emission properties were summarized by B+80, who also noted that a third maser (H_2O 351·24+0·66) with no OH counterpart is present and exhibits exceptionally strong high-velocity emission (see also Rodriguez *et al.* 1978).

H_2O 351·58−0·36 (*Fig. 2*). This new H_2O maser and its OH maser counterpart are associated with a compact HII region and are at a distance of ~10 kpc. High-velocity emission is present at $v = -72$ km s^{-1}.

H_2O 351·77−0·54 (*Fig. 2*). This H_2O maser coincides with an OH maser which is currently the strongest known (Caswell and Haynes 1980, 1983). Our H_2O spectrum for 1981 December is generally similar to the discovery spectrum taken by Braz and Scalise (1982) in 1980 October and shows several weak features in the velocity range −27 to +20 km s^{-1}, with the strongest feature at −1 km s^{-1} coinciding with the velocity of the strongest OH feature. Fix *et al.* (1982) showed an H_2O spectrum obtained in 1981 April in which the major feature is the same and the weaker features cover a similar velocity range but differ in detail. Fix *et al.* also gave an OH position of $17^h\,23^m\,20^s{\cdot}5$, $-36°\,06'\,45''$ (error not quoted) which differs by $<5''$ arc from the lower precision measurement of Caswell and Haynes (1980). Our H_2O position (Table 1) is the best currently available and the offset from the OH position is $<10''$ arc and not significant. The nearby continuum source with a flux density of 0·3 Jy (Haynes *et al.* 1978; Caswell and Haynes 1980) has been mapped at high resolution by Fix *et al.*, who found it to be significantly offset from the OH position (by 12″ arc). A much weaker source with flux density not quoted by Fix *et al.* (but apparently <3 mJy) coincides with the OH maser. The extensive molecular cloud in the region, inferred by Caswell and Haynes (1980, 1983) on the basis of OH satellite-line extended absorption and emission, is confirmed by the CO detection reported by Fix *et al.*

It seems likely that the large intensity ratio of OH emission to IR emission (Braz and Epchtein 1982) should place valuable constraints on OH pumping models. The question of whether there is a small position offset between the OH and H_2O masers also needs to be resolved.

H_2O 352·52−0·16 (*Fig. 2*). The new H_2O maser is weak and shows two features near $v = -50$ km s^{-1}, a velocity similar to that of the OH maser 352·51−0·15. An HII region in this direction has $v = -82$ km s^{-1} and is presumably *not* related to the masers.

H_2O 353·41−0·36. This was discovered by B+80; no new observations were made.

H_2O 353·46+0·55. This weak new H_2O maser is associated with an OH maser showing 1665 and 1612 MHz emission but not 1667 MHz emission.

H_2O 354·61+0·47 (*Fig. 2*). This new H_2O maser is associated with an OH maser and HII region.

H_2O 355·34+0·14 (*Fig. 2*). A weak detection at <3 Jy in 1978 September was reported by Scalise and Braz (1980); our measurement in 1981 December now

shows a strong source with peak intensity of 59 Jy and several subsidiary peaks. The associated OH maser is quite strong and a diffuse HII region may be associated. The kinematic distance of ~20 kpc may be incorrect and a nearby position (~2 kpc) with non-circular motions present may be a better estimate.

H_2O 356·64−0·33. Emission at $v = -10$ and -2 km s^{-1} was discovered by B+80; no new observations were made. The associated OH maser may be circumstellar emission from a late-type star (CH 83) and is probably to be identified with IRC-30308.

H_2O 358·23+0·11 (*Fig. 3*). This is a new H_2O maser with many features filling the range -29 to $+13$ km s^{-1}. The corresponding OH maser is detectable at 1612, 1665 and 1667 MHz and shows emission from -32 to $+19$ km s^{-1}, resembling the circumstellar emission from late-type stars.

H_2O 358·67−0·05 (*Fig. 3*). This is a new H_2O maser with features filling the range -28 to 0 km s^{-1} and extending as far as $+26$ km s^{-1}; possibly the baseline is curved and hence we cannot be certain that the emission is continuous between 0 and $+26$ km s^{-1}. The corresponding OH maser is detectable at 1612, 1665 and 1667 MHz and shows emission from $v = -32$ to $+29$ km s^{-1}; like the previous source, this maser is probably associated with the circumstellar envelope of a late-type star.

H_2O 359·14+0·03 (*Fig. 3*). One of the strongest sources among our new discoveries, this H_2O maser shows several high-velocity features over the range $v = -33$ to $+13$ km s^{-1}.

H_2O 359·43−0·11 (*Fig. 3*). The velocity of this new H_2O maser (and its OH counterpart) indicates a location near the galactic centre.

H_2O 359·62−0·25 (*Fig. 3*). This is one of the few new H_2O masers for which we have two epoch observations. The 12 Jy feature near $v = +13$ km s^{-1} was present in both 1981 December and 1982 April but at $v = +9$ km s^{-1} a 42 Jy feature in 1981 December had 'disappeared' (<3 Jy) by 1982 April. High-velocity features of ~2 Jy are just detectable near $v = +25$ and $+39$ km s^{-1} at both epochs. The location of this source and its OH maser counterpart is probably near the galactic centre.

H_2O 359·97−0·46 (*Fig. 3*). This is a new H_2O and OH maser pair, probably located near the galactic centre.

H_2O 0·37+0·04 (*Fig. 3*). This is also a new H_2O and OH maser pair, probably located near the galactic centre.

H_2O 0·54−0·85. Previous observations were summarized by B+80; a current spectrum (1981 December) still shows many high-velocity features extending from -55 to $+91$ km s^{-1}, with intensities of ~20 Jy; however, the three main features are much stronger, being 310 Jy at $+15$ km s^{-1}, 470 Jy at $+18{\cdot}5$ km s^{-1} and 210 Jy at $+32$ km s^{-1}, compared with peaks of <60 Jy in 1977. Despite its longitude near the galactic centre, this source is possibly at a distance of only a few kpc since the associated HII region is visible.

H_2O 0·66−0·04. This is the well-known H_2O maser in Sgr B2 which is a rich source of many molecular species located near the galactic centre.

H_2O 2·14+0·01 (*Fig. 3*). This is a new H_2O maser showing a single feature which has increased from 10 to 15 Jy in the period 1981 December to 1982 April.

OH Sources with No H_2O Detected

OH340·78−0·10. The velocity structure of this OH maser is suggestive of a shell; its mean velocity indicates a kinematic distance near the tangential point, at 9·4 kpc. 1720 MHz emission is present; no significant HII region is detectable.

OH341·27+0·07. This OH maser is weak and has no detectable continuum emission; it may be at the far kinematic distance (12·7 kpc) rather than the near distance (6·3 kpc).

OH344·41+0·05, OH346·48+0·13 and OH347·87+0·01. These OH masers are quite weak single features detected at 1665 MHz.

OH348·89+0·09. A distant ($\geqslant$8·9 kpc) OH maser with no detectable HII region near it. Weak (1·9 Jy) H_2O emission with $v = -78$ km s^{-1} may be present in our 1981 December observations but is not reliably above the noise level.

OH352·16+0·21. This is a weak OH maser with no detectable continuum emission associated.

OH356·66−0·27. This is a quite weak OH maser, with a velocity indicating a location near the galactic centre.

4. Discussion

High-velocity Emission

Ten of the H_2O masers in this longitude range show high-velocity emission. The most dramatic is H_2O 351·24+0·66 (Rodriguez *et al.* 1978; B+80), in which the high-velocity emission is more intense than the low-velocity emission. In the more usual situation, high-velocity emission intensities are between 1% and 10% of the main velocity emission, and consequently for many of our weak new sources high-velocity emission at such a low level would have been below our detection limit.

Galactic Distribution

Since the search was conducted at the positions of OH masers and since the majority of the search positions yielded an H_2O maser, the distribution is necessarily similar to that of the OH masers (see CH 83). In the case of the OH masers, CH 83 derived a galactic distribution which peaked between galactic radii of 5 and 8·5 kpc (see p. 393). A similar distribution may apply to the H_2O masers but a correct derivation of such a distribution will only be possible when an unbiased search for H_2O masers has been conducted down to well-defined sensitivity levels.

However, there seems no doubt that the galactic centre is *not* deficient in H_2O sources, contrary to the assertion of Genzel and Downes (1979). They were aware of only one H_2O maser (Sgr B2) within the central 500 pc of our galaxy; our OH survey revealed at least five such OH masers (including Sgr B2) and for four of these we have now detected H_2O masers. Indeed, far from a deficiency of H_2O masers, there appears to be a local maximum of star formation regions (as defined by OH/H_2O masers) near the galactic centre.

Luminosity Function

The luminosity function of H_2O masers has been discussed by Johnston *et al.* (1973) and Genzel and Downes (1977). Both groups found a median luminosity near

$10^{29.5}$ erg s^{-1} (equivalent to a 10 Jy peak averaged over 4 km s^{-1} at a distance of 10 kpc). This, significantly, corresponds roughly to the sensitivity limit of most surveys to date. Provided that the search directions are representative of all varieties of strong H_2O masers the shape of the distribution above this median value should be valid. Below the median value the raw distribution is dominated by sensitivity effects which have not been evaluated and it is completely unknown at what luminosity the function begins to decrease. For *OH masers* however a luminosity function has been derived (CH 83, p. 395), which allows for sensitivity limits, and a similar approach is needed for the H_2O masers. We are currently extending our survey to increase the data base available for such an analysis.

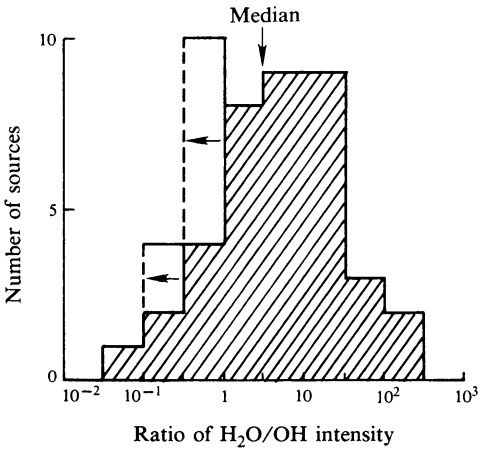

Fig. 4. Distribution of the ratio of peak H_2O flux density to peak flux density of the associated OH maser. The hatched area corresponds to detected H_2O counterparts, the unhatched area to H_2O upper limits.

Association with OH Masers

Overall we have discovered H_2O masers at 80% of the type I OH maser sites, which is a success rate much higher than previously achieved. The question of whether even the 20% non-detections are largely due to sensitivity limitations is complicated by the range of distances involved (which modify the received flux density by factors of up to 10^3), and it is useful to make some distance-independent comparison. For this purpose we study the ratio of peak H_2O flux density to peak OH flux density (since the peak flux density is the simplest intensity measure and is directly related to the sensitivity limit). The histogram showing the distribution of this ratio is shown in Fig. 4. The median is found to be ~ 3 and the scatter can be described (approximately, since upper limits are present below the median value) by a standard deviation of about one order of magnitude. When we look at the distribution of upper limits we see that they lie well within the distribution defined by the detected H_2O masers and provide no evidence for a distinct class of OH masers without H_2O counterparts; indeed many new detections would probably result from a slightly deeper H_2O search and, in view of the erratic short-term variability of H_2O masers, even a search at a different epoch would probably yield additional detections.

Thus there is no doubt that the OH maser sites are amongst the locations in the Galaxy most likely to yield an H_2O maser and the association approaches a one-to-one correspondence. The velocity ranges of OH and H_2O emission generally overlap but there is no agreement in detail. For most of the OH/H_2O maser pairs in Table 1 the positions are coincident within the error limits of typically 30″ arc; measurements

of greater precision are now needed to ascertain just how good is the coincidence. Continuum measurements of high resolution and high sensitivity are also needed in order to search for associated HII regions. Early OH searches (and subsequent H_2O searches) which concentrated on strong well-developed HII regions gave a misleading bias to the distribution of maser sites, and it is now clear that many of the OH/H_2O masers are not near any strong HII regions. However, most are believed to be associated with very young and compact, but weak, HII regions (see e.g. Habing *et al.* 1974).

We now ask what the nature is of the H_2O/OH association. The possibilities include: (i) a close correspondence, with both types of maser present in the envelope of a single star; (ii) a loose correspondence, whereby the OH and H_2O masers may occur at different phases in star formation and any association is merely an indication of the presence of several objects at various stages of evolution.

Possibility (i) provides a simple and attractive explanation for the associations. However, this model encounters difficulties in explaining the small but significant offset between OH and H_2O masers found in several instances where high-precision positions have been measured (see e.g. Forster *et al.* 1978; Norris *et al.* 1980); such detailed position information is at present available for only a few OH/H_2O pairs, but if such offsets prove to be common then it would argue strongly against both types of maser being present in a common envelope. (Although the OH and H_2O masers might well occur at different radial distances from the core, this would lead to roughly concentric distributions rather than a simple displacement between the OH and H_2O centroids.)

Possibility (ii) seems unlikely, since the approximate one-to-one correspondence which we find would then be highly improbable. Our present systematic search of a large sample of OH masers suggests that *groups* of OH and H_2O masers on a scale of 10″ arc to 100″ arc are quite rare. Here again the histogram of intensity ratios is useful, since we can use the median as an unbiased quantitative assessment of whether a second, displaced, H_2O maser is present. In most cases we can exclude the possibility that there is a second H_2O maser with an H_2O/OH intensity ratio exceeding the median value.

So what can the nature be of an association which tends to yield a roughly one-to-one correspondence yet sometimes appears to suggest an abhorrence of precise coincidences? The implication is that the objects occur in pairs (rather than either singly or in clusters); this could most simply be explained if the typical star formation process generates two major fragments, one being seen as the new star with a compact HII region and an OH maser in its outer envelope, and the other remaining for some time as a very dense, compact, cool molecular cloud. This latter object may be the principal site of the H_2O emission, with smaller fragments in the vicinity accounting for the medium-velocity to high-velocity 'ejecta' often seen. Speculations in this vein have made been by Shull (1982), whose main objective was to account for the high-velocity ejecta, of relatively small mass, as matter expelled in the star-forming process. Our major development of this picture is to suggest that the fragmentation also leads to *a principal blob*, of star-like mass, which is the dominant source of H_2O maser emission. Such a binary process in star formation has often been invoked as a means of shedding excess angular momentum. The existence of high-intensity H_2O maser emission from fast-moving ejecta (for example $H_2O\,351{\cdot}24{+}0{\cdot}66$) suggests that the maser pumping mechanism does not require a developed star within

the masing blob, and that the conditions of high density, suitable molecular abundances and appropriate temperature may suffice. Details of H_2O maser pump schemes are still very uncertain (see e.g. Deguchi 1981), but if the H_2O maser pump is quite modest in its requirements, then one might expect there to be a considerable number of H_2O masers with no related OH maser; attempts to verify this must await more extensive H_2O surveys.

To further assess the above binary model of OH/H_2O maser associations, increased emphasis must be given on the observational side to more accurate position comparisons. An occasional precise coincidence of OH and H_2O masers is compatible with our speculation, and likewise the occasional cluster of masers in very active regions of star formation will inevitably occur; in the case of OH/H_2O pairs which are fairly isolated, with no prominent HII region nearby, it will be especially important to determine whether there are small but significant offsets between the OH and H_2O masers.

References

Batchelor, R. A., Caswell, J. L., Goss, W. M., Haynes, R. F., Knowles, S. H., and Wellington, K. J. (1980). *Aust. J. Phys.* **33**, 139.

Braz, M. A., and Epchtein, N. (1982). *Astron. Astrophys.* **111**, 91.

Braz, M. A., and Scalise, E. (1982). *Astron. Astrophys.* **107**, 272.

Caswell, J. L., and Haynes, R. F. (1980). IAU Circular No. 3509.

Caswell, J. L., and Haynes, R. F. (1983). *Aust. J. Phys.* **36**, 361.

Caswell, J. L., Haynes, R. F., Goss, W. M., and Mebold, U. (1981). *Aust. J. Phys.* **34**, 333.

Deguchi, S. (1981). *Astrophys. J.* **249**, 145.

Fix, J. D., Mutel, R. L., Gaume, R. A., and Claussen, M. J. (1982). *Astrophys. J.* **259**, 657.

Forster, J. R., Welch, W. J., Wright, M. C. H., and Baudry, A. (1978). *Astrophys. J.* **221**, 137.

Genzel, R., and Downes, D. (1977). *Astron. Astrophys. Suppl.* **30**, 145.

Genzel, R., and Downes, D. (1979). *Astron. Astrophys.* **72**, 234.

Habing, H. J., Goss, W. M., Matthews, H. E., and Winnberg, A. (1974). *Astron. Astrophys.* **35**, 1.

Haynes, R. F., Caswell, J. L., and Simons, L. W. J. (1978). *Aust. J. Phys. Astrophys. Suppl.* No. 45, 1.

Johnston, K. J., Sloanaker, R. M., and Bologna, J. M. (1973). *Astrophys. J.* **182**, 67.

Kaufmann, P., Zisk, S., Scalise, E., Schaal, R. E., and Gammon, R. H. (1977). *Astron. J.* **82**, 577.

Knowles, S. H., and Batchelor, R. A. (1978). *Mon. Not. R. Astron. Soc.* **184**, 107.

Norris, R. P., Booth, R. S., and Davis, R. J. (1980). *Mon. Not. R. Astron. Soc.* **190**, 163.

Rodriguez, L. F., Moran, J. M., Dickinson, D. F., and Gyulbudaghian, A. L. (1978). *Astrophys. J.* **226**, 115.

Sandell, G., Scalise, E., and Braz, M. A. (1983). *Astron. Astrophys.* (in press).

Scalise, E., and Braz, M. A. (1980). *Astron. Astrophys.* **85**, 149.

Shull, M. J. (1982). *In* 'Regions of Recent Star Formation' (Eds R. S. Roger and P. E. Dewdney), p. 91 (Reidel: Dordrecht).

Turner, B. E. (1970). *Astrophys. Lett.* **6**, 99.

Turner, B. E. (1979). *Astron. Astrophys. Suppl.* **37**, 1.

Manuscript received 1 November 1982, accepted 16 February 1983